# Hydrocarbon ions in fuel-rich, $CH_4$–$C_2H_2$–$O_2$ flames as a probe for the initiation of soot: interpretation of the ion chemistry

JOHN M. GOODINGS, SCOTT D. TANNER,[1] AND DIETHARD K. BOHME
*York University, Department of Chemistry, 4700 Keele Street, Downsview, Ont., Canada M3J 1P3*

Received March 25, 1982

JOHN M. GOODINGS, SCOTT D. TANNER, and DIETHARD K. BOHME. Can. J. Chem. **60**, 2766 (1982).

The ion chemistry is discussed for fuel-rich, nearly sooting, methane–oxygen flames at atmospheric pressure with added acetylene. Different types of ion–molecule reactions, both positive and negative, which can contribute through chemical ionization (CI) processes are summarized including their dependence on temperature, pressure, and equivalence ratio $\phi$. Extensive data were presented previously involving ion concentration profiles measured with a mass spectrometer as a function of distance along the axis of conical flames. An understanding of the dominant CI processes provides insight into the early chemical stage of soot formation associated with the flame reaction zone. The negative ion profiles show moderately unsaturated hydrocarbon ions upstream formed by proton transfer followed by progressive dehydrogenation; the highly unsaturated, carbonaceous ions observed downstream appear to arise by two- and three-body electron attachment, charge transfer, and H-atom stripping. The negative hydrocarbon ions can all be explained in terms of polyacetylene derivatives. The same build-up of carbonaceous species downstream is evident from the positive ion profiles. A major role is ascribed to proton transfer reactions with lesser contributions from charge transfer and ion–molecule condensation; three-body association is probably insignificant. Experiments with added acetylene indicate extensive fuel pyrolysis early in the reaction zone. There is no evidence that an ionic mechanism is dominant in forming soot precursors compared with neutral condensation reactions. Because of complexities in the positive ion chemistry, the negative ions appear to provide the more straightforward probe of the underlying neutral chemistry.

JOHN M. GOODINGS, SCOTT D. TANNER et DIETHARD K. BOHME. Can. J. Chem. **60**, 2766 (1982).

On discute de la chimie ionique dans les flammes du méthane–oxygène riches en combustible et sur le point de former de la suie, auxquelles on a ajouté de l'acétylène et à la pression atmosphérique. On classifie les différents types de réactions ion–molécule, tant positives que négatives qui peuvent contribuer via des processus d'ionisation chimique (IC) et on inclut également l'effet de la température, de la pression et du rapport d'équivalence $\phi$ sur ces réactions. On a présenté antérieurement de nombreuses données impliquant les profils de concentration des ions mesurés à l'aide d'un spectromètre de masse en fonction de la distance le long de flammes coniques. Une compréhension des processus IC dominant fournit un renseignement au sujet de la première étape de formation de la suie associée à la zone de réaction de flamme. Les profils de l'ion négatif montrent que, près de la flamme, on retrouve des ions d'hydrocarbonés modérement insaturés qui se forment par un transfert de proton suivi d'une déshydrogénation progressive. Les ions carbonés hautement insaturés observés plus loin semblent provenir de liaisons électroniques à deux et trois composantes saturées, de transferts de charge et de l'élimination d'atomes d'hydrogène. On peut expliquer les ions carbonés négatifs en termes de dérivés polyacétyléniques. La même accumulation d'espèces carbonés loin de la flamme peut être mise en évidence à partir des profils des ions positifs. On attribue un rôle prépondérant aux réactions de transfert de proton accompagné de contributions moindres de transferts de charge et de condensations ion–molécule: une association à trois composantes n'est probablement pas importante. Les expériences conduites avec de l'acétylène ajouté indiquent une abondante pyrolyse du carburant se produisant très tôt dans la zone de réaction. Il n'y a pas de preuve d'un mécanisme ionique dominant lors de la formation des précurseurs de suie par comparaison avec les réactions neutres de condensation. A cause de la complexité de la chimie de l'ion positif, les ions négatifs apparaissent comme les meilleures guides pour étudier la chimie neutre sous jacente.

[Traduit par le journal]

## Introduction

In a recent article (1), here designated as paper I, we reported experimental data on the axial distribution of both positive and negative ions monitored directly through the reaction zones of fuel-rich $CH_4$–$C_2H_2$–$O_2$ flames at atmospheric pressure. The natural hydrocarbon ions $C_nH_x^{\pm}$ were studied as a probe of the early chemical stages of soot formation. In that paper, the phenomenological changes in the ion distribution which accompanied changes in the equivalence ratio $\phi$ and temperature were noted. In this report we interpret the previous data from the point of view of the ion–molecule reaction chemistry. It is hoped that an understanding of the kinetics and energetics of the ion–molecule reactions responsible for the observed flame-ion distribution will lead to further insights into the initial chemistry leading to soot.

The types of reactions commonly thought to dominate the ion chemistry of flames have been conveniently classified. Those processes which result in the ionization of neutral flame intermediates include chemi-ionization, thermal ionization, electron attachment, charge transfer, and proton-transfer. The latter four reaction types share the characteristic that the neutral reactant of molecular weight $M$ is converted in most cases to an ion of $m/e = M^{\pm}$, $(M + 1)^{+}$, or $(M - 1)^{-}$. As a result, the identification of the neutral precursors from the ion

---

[1] Present address: Sciex Inc., 55 Glencameron Road, #202, Thornhill, Ont., Canada L3T 1P2.

0008-4042/82/222766-11$01.00/0

spectrum is relatively simple for systems in which these reaction types predominate. More difficult to deconvolute is the spectrum resulting from "ionic polymerization" reactions such as condensation and three-body association.

## Types of ion–molecule reactions relevant to hydrocarbon flame chemistry

A considerable data base on the kinetics of relevant hydrocarbon ion–molecule reactions exists. However, most of the kinetic measurements have been performed at or near room temperature and at low pressure. This section presents an overview of our current understanding of the kinetics of ion–neutral reactions involving hydrocarbon molecules and radicals. To facilitate the application of the data base to flames burning at atmospheric pressure, the dependence of the kinetics of the major reaction types on temperature ($T$) and pressure ($P$) is reviewed.

### *1. Chemi-ionization*

Neutral reactions leading to the formation of ions are usually endothermic. Exceptions may arise when the reactants are radicals and electronically-excited molecules, the concentrations of which will show a strong positive $T$-dependence. It is now generally agreed that the major source of natural flame ions is the chemi-ionization reaction (2, 3)

[1] $CH + O \rightarrow CHO^+ + e^-$

Of those chemi-ionization reactions which yield directly a hydrocarbon ion, the most frequently cited are

[2] $CH^* + C_2H_2 \rightarrow C_3H_3^+ + e^-$

[3] $CH^* + C_2H_4 \rightarrow C_3H_5^+ + e^-$

However, these latter sources have been discounted as anything but minor contributors to the total ion density (4). No $P$-dependence is expected for chemi-ionization reactions, except for the possible quenching of excited reactants.

### *2. Thermal ionization*

The spontaneous ionization of energetic molecules may be regarded as a quasi-unimolecular Lindemann process

[4*a*] $C_nH_x + M \rightarrow (C_nH_x)^* + M$

[4*b*] $(C_nH_x)^* \rightarrow C_nH_x^+ + e^-$

In the high pressure limit, appropriate for thermal ionization in atmospheric pressure flames, the classical RRK treatment (5) yields an Arrhenius-type unimolecular rate constant

$$k = \nu \exp(-E_a/RT)$$

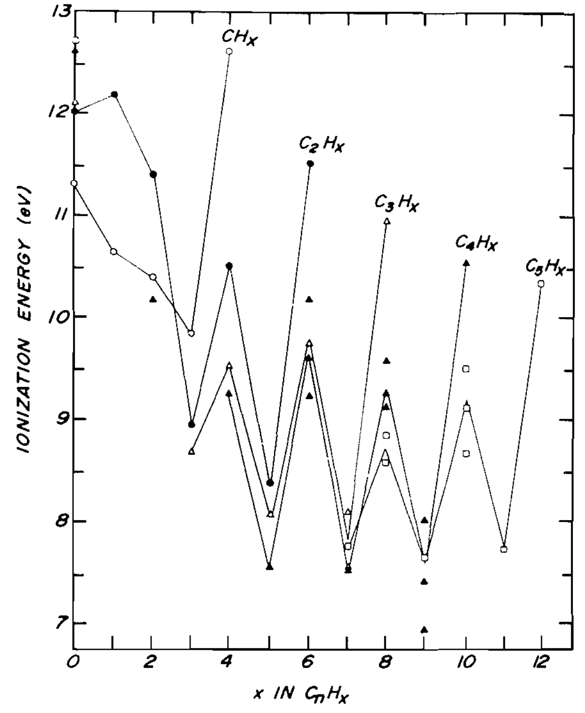

FIG. 1. Ionization energies of aliphatic hydrocarbon radicals and molecules. In cases where data for several isomers are shown, the line is drawn through the arithmetic mean of the ionization energies.

where $\nu$ is typically $10^{13}$ to $10^{15}$ $s^{-1}$ and the activation energy $E_a$ is approximately the ionization energy IE of $C_nH_x$. The IE's of aliphatic $C_nH_x$ radicals and molecules show remarkable trends with the parity of $x$ and magnitude of $n$, as given in Fig. 1. The obvious feature is the alternation of IE with $x$; IE's of odd-$x$ species are roughly 1.5 eV lower than those of similar species with even-$x$. Also, the IE tends to decrease with increasing $n$ (except for $x = 0$). It is assumed that the thermal ionization process is pressure-saturated for an atmospheric pressure flame.

### *3. Proton transfer*

These reactions are frequently observed to be simple and fast. Examples include

[5] $HCO^+ + C_2H_2 \rightarrow C_2H_3^+ + CO$

[6] $OH^- + CH_3C_2H \rightarrow C_3H_3^- + H_2O$

for which these were the only reaction channels observed (6, 7), and the rate constants were large, $(1.4 \pm 0.4) \times 10^{-9}$ and $(1.7 \pm 0.3) \times 10^{-9}$ $cm^3$ $molecule^{-1}$ $s^{-1}$, respectively. In fact, the rate constants for proton transfer reactions are generally found to be well-approximated by the AADO

TABLE 1. Proton affinities, PA$^\circ_{298}$ in kJ mol$^{-1}$, for some hydrocarbon flame species in order of decreasing PA$^a$

| Ion | Molecule | PA | Ref. | Ion | Molecule | PA | Ref. |
|---|---|---|---|---|---|---|---|
| $C_5H_7^+$ | Cyclopentadiene | 837 | 9 | $C_4H_3^+$ | Diacetylene | 724 | 10 |
| $CH_3^+$ | $CH_2$ | 828 | 10 | $CH_3O^+$ | Formaldehyde | 715 | 14 |
| $C_4H_7^+$ | Isobutene | 812 | 9 | $C_4H_{11}^+$ | Isobutane | 699 | 9 |
| $C_2H_3O^+$ | Ketene | 807 | 11 | $H_3O^+$ | Water | 692 | 15 |
| $C_7H_9^+$ | Toluene | 787 | 9 | $C_2H_5^+$ | Ethylene | 682 | 15 |
| $C_3H_5^+$ | Allene | 778 | 10 | $C_2H_2^+$ | $C_2H$ | 682 | 10 |
| $C_3H_5^+$ | Methylacetylene | 770 | 10 | $C_2H_3^+$ | Acetylene | 636 | 10 |
| $C_4H_7^+$ | 1-Butene | 766 | 9 | $CH^+$ | Carbon | 628 | 10 |
| $C_4H_7^+$ | *cis*-2-Butene | 757 | 9 | $C_3H_9^+$ | Propane | 619 | 9 |
| $CH_5O^+$ | Methanol | 757 | 12 | $C_2H_6^+$ | Ethyl radical | 602 | 10 |
| $C_4H_7^+$ | *trans*-2-Butene | 753 | 9 | $C_2H_7^+$ | Ethane | 595 | 15 |
| $C_3H_7^+$ | Propene | 753 | 12 | $CHO^+$ | Carbon monoxide | 592 | 16 |
| $C_6H_7^+$ | Benzene | 753 | 9 | $CH_5^+$ | Methane | 546 | 16 |
| $C_5H_9^+$ | Cyclopentene | 745 | 9 | $CHO_2^+$ | Carbon dioxide | 538 | 16 |
| $C_2H^+$ | $C_2$ | 732 | 10, 13 | $CH_4^+$ | Methyl radical | 529 | 10 |
| $CH_2^+$ | CH | 728 | 10 | | | | |

[a] The PA's of some important flame ions containing oxygen are included as benchmarks.

ion–molecule collision theory of Su, Su, and Bowers (8). This theory predicts reactions involving non-polar species to be temperature-independent, while reactions involving very polar species can be expected to approach a $T^{-1/2}$-dependence. It is commonly the case that proton transfer will take place if it is exothermic. The data base of proton affinities for aliphatic hydrocarbons is rather scant; some relevent values that have been reported are listed in Table 1. Occasionally, an exothermic proton transfer process is observed to compete (with varying success) with other reaction channels. Such is the case for the reaction

$$[7] \quad O^- + C_2H_2 \xrightarrow{0.6} e^- + C_2H_2O$$
$$\xrightarrow{0.3} C_2H^- + OH$$
$$\xrightarrow{0.05} HC_2O^- + H$$
$$\xrightarrow{0.05} C_2^- + H_2O$$

which, nonetheless, has the large overall rate constant $(2.0 \pm 0.3) \times 10^{-9}$ cm$^3$ molecule$^{-1}$ s$^{-1}$ (17). Finally, dissociative proton transfer, in which the product ion breaks up in a unimolecular process, is frequently observed in reactions for which the simple proton transfer is sufficiently exothermic, for example (18),

$$[8] \quad CH_5^+ + C_2H_6 \rightarrow C_2H_7^+ + CH_4$$
$$\rightarrow C_2H_5^+ + CH_4 + H_2$$

Since it is expected that the proton affinities of $C_nH_x$ species increase with $n$, more pronounced dissociation of the proton transfer product ion may occur for the larger hydrocarbons. The overall rate constant is not expected to be $P$-dependent. However, the branching ratio may show $P$-dependence depending on the lifetime of the ionic collision complex.

### 4. *Charge transfer*

The rate constants for many charge transfer reactions involving simple species are also often found to be in good agreement with the predictions of the AADO collision theory. However, in such cases two conditions are usually met: (*a*) the reactants are polyatomics (since the requirement for energy resonance is more easily fulfilled when there is a high density of states); and (*b*) other reaction channels, such as proton transfer and condensation, are not competitive. The latter requirement appears to be more difficult to satisfy for charge transfer reactions involving hydrocarbons; we are not aware of any example in the published literature. Examples of charge transfer to a hydrocarbon proceeding in isolation but involving dissociation are known, however. The thermochemistry which governs these reactions involves the ionization energies of the reactants, and so the data of Fig. 1 apply here as well. The rates of charge transfer reactions, when efficient, are expected to show only a weak $T^{-1/2}$-dependence and no $P$-dependence.

### 5. *Condensation*

Reactions in which new bonds between heavy atoms (e.g. C, O) are formed are termed condensation reactions. Examples which have been reported may be separated into two classes which are defined by the observed kinetics. The rate constants for condensation reactions which are rapid at room temperature are usually well-approximated by the AADO collision theory. Some of these reactions are slow at room temperature and may be

TABLE 2. Reactions of positive hydrocarbon ions with methane measured at room temperature

$$\begin{array}{l}
\left.\begin{array}{lll}
C_nH_x^+ + CH_4 & \longrightarrow C_{n+1}H_{x+1}^+ + H_2 + H & (a) \\
 & \longrightarrow C_{n+1}H_{x+2}^+ + H_2 & (b) \\
 & \longrightarrow C_{n+1}H_{x+3}^+ + H & (c) \\
 & \xrightarrow{M} C_{n+1}H_{x+4}^+ & (d)
\end{array}\right\} \begin{array}{l}\text{Condensation} \\ \\ \text{(3-body association)}\end{array} \\
\begin{array}{llll}
\phantom{C_nH_x^+ + CH_4} & \longrightarrow C_nH_{x+1}^+ + CH_3 & (e) & \text{H-transfer} \\
 & \longrightarrow C_nH_{x+2}^+ + CH_2 & (f) & \text{H}_2\text{-transfer}
\end{array}
\end{array}$$

| $C_nH_x^+$ | (*a*) | (*b*) | (*c*) | (*d*) | (*e*) | (*f*) | $k$ ($\times 10^{-9}$)[a] | Ref. |
|---|---|---|---|---|---|---|---|---|
| $C^+$ | | √ | √ | | | | 1.2 | 19, 20, 21 |
| $CH^+$ | √ | √ | √ | | | | 1.3 | 19, 21 |
| $CH_2^+$ | | √ | √ | | | | 1.2 | 19, 21 |
| $CH_3^+$ | | √ | | | | | 1.2 | 19, 22 |
| $CH_4^+$ | | | | | √ | | 1.5 | 22 |
| $C_2^+$ | √ | √ | √ | | √ | √ | 1.4 | 19 |
| $C_2H^+$ | | √ | √ | √ | √ | | 1.1 | 19 |
| $C_2H_2^+$ | | √ | √ | | | | 1.0 | 19 |
| $C_2H_3^+$ | | √ | | | | | 0.17 | 19, 21 |
| $C_2H_4^+$ | | | | | | | $<0.0001$ | 19 |

[a]Rate constants in units of $cm^3$ $molecule^{-1}$ $s^{-1}$.

TABLE 3. Reactions of positive hydrocarbon ions with acetylene measured at room temperature

$$\begin{array}{l}
\left.\begin{array}{lll}
C_nH_x^+ + C_2H_2 & \longrightarrow C_{n+2}H_x^+ + H_2 & (g) \\
 & \longrightarrow C_{n+2}H_{x+1}^+ + H & (h) \\
 & \xrightarrow{M} C_nH_x^+ \cdot C_2H_2 & (i) \\
 & \longrightarrow C_{n+1}H_{x-2}^+ + CH_4 & (j)
\end{array}\right] \begin{array}{l}\text{Condensation} \\ \text{(3-body association)} \\ \\ \end{array} \\
\begin{array}{llll}
\phantom{C_nH_x^+ + C_2H_2} & \longrightarrow C_2H_3^+ + C_nH_{x-1} & (m) & \text{Proton transfer}
\end{array}
\end{array}$$

| $C_nH_x^+$ | (*g*) | (*h*) | (*i*) | (*j*) | (*m*) | $k$ ($\times 10^{-9}$)[a] | $k$ ($\times 10^{-25}$)[b] | Ref. |
|---|---|---|---|---|---|---|---|---|
| $CH^+$ | | | | | √ | 0.8 | | 21 |
| $CH_3^+$ | √ | | | | | 1.2 | | 23 |
| $CH_5^+$ | | | | | √ | 1.56 | | 6 |
| $C_2^+$ | | √ | | | | 3, 2.65 | | 21 |
| $C_2H^+$ | | √ | | | √ | 2.4, 1.47, 2.45, 1.3 | | 21 |
| $C_2H_2^+$ | √ | √ | | | | 1.15, 1.52, 1.22, 0.90, 0.79, 0.33 | | 21 |
| | √ | √ | √ | | | 1.39 | | |
| | √ | √ | √ | | √ | 1.25 | | |
| | √ | √ | | | √ | 1.94, 1.41 | | |
| $C_2H_3^+$ | | | √ | | | | 2.98 ($H_2$) | 24 |
| | | | | | | 0.71, 0.085, 0.31[c] | | 21 |
| $C_2H_5^+$ | | | √ | | | | 1.34 ($H_2$) | 24 |
| | | | | √ | | 0.0075 | | 24 |
| $C_2H_6^+$ | | | | | | 0.10, 1.4[c] | | 21 |

[a]Rate constants in units of $cm^3$ $molecule^{-1}$ $s^{-1}$.
[b]Rate constants in units of $cm^6$ $molecule^{-2}$ $s^{-1}$.
[c]Product ions not given.

expected to show a *T*-dependence which is positive. Many examples are provided in the summaries given in Tables 2 and 3 for reactions of hydrocarbon ions with $CH_4$ and $C_2H_2$, respectively. Reactions of these ions with $H_2$, a major product in fuel-rich flames, are summarized in Table 4. One representative of the first type of condensation reactions is (23)

[9] $CH_3^+ + C_2H_2 \rightarrow C_3H_3^+ + H_2$

which is rapid ($1.2 \times 10^{-9}$ $cm^3$ $molecule^{-1}$ $s^{-1}$) and no other products were observed. By the same token, the reaction (19, 21)

[10] $C_2H_3^+ + CH_4 \rightarrow C_3H_5^+ + H_2$

is slow ($0.17 \times 10^{-9}$ $cm^3$ $molecule^{-1}$ $s^{-1}$) which probably places it in the category of reactions

TABLE 4. Reactions of positive hydrocarbon ions with hydrogen measured at room temperature unless otherwise noted

$$C_nH_x^+ + H_2 \longrightarrow C_nH_{x+1}^+ + H \quad (n)$$
$$\xrightarrow{M} C_nH_{x+2}^+ \quad (p)$$

| $C_nH_x^+$ | ($n$) | ($p$) | $k$ ($\times 10^{-9}$)[a] | $k$ ($\times 10^{-27}$)[b] | Ref. |
|---|---|---|---|---|---|
| $C^+$ | | √ | $<0.0005$ | 0.021 (He)[c] | 25, 26 |
| $CH^+$ | √ | | 1.2 | | 25 |
| $CH_2^+$ | √ | | 1.6 | | 25 |
| $CH_3^+$ | | √ | | 0.13 (He)[d] | 25 |
| $CH_4^+$ | √ | | 0.033 | | 25 |
| $C_2^+$ | √ | | 1.4 | | 25 |
| $C_2H^+$ | √ | | 1.7 | | 25 |
| $C_2H_2^+$ | √ | √ | 0.010 | 1.2 (He) | 25 |
| $C_2H_3^+$ | | √ | | 0.02 (He) | 25 |
| | | | | 0.015 ($H_2$) | 24 |
| $C_2H_4^+$ | | | $<0.00004$ | | 25 |
| $C_2H_5^+$ | | | $<0.00004$ | | 25 |

[a] Rate constants in units of $cm^3$ molecule$^{-1}$ $s^{-1}$.
[b] Rate constants in units of $cm^6$ molecule$^{-2}$ $s^{-1}$.
[c] Measured at 90 K.
[d] Measured in the temperature range 225–300 K.

having an activation energy. Condensation reactions are not necessarily limited to positive ions; the somewhat special case of associative detachment may be thought of as negative ion condensation. An example which competes successfully with proton transfer has already been presented in [7] involving the reaction of $O^-$ with acetylene where the condensation product is uncharged (17). Also, room-temperature studies of reactions of $C_2^-$ and $C_2H^-$ with $CH_4$ and $C_2H_2$ (27) failed to reveal any condensation products ($k$'s $< 10^{-13}$ $cm^3$ molecule$^{-1}$ $s^{-1}$).

### 6. *Three-body association*

Ion–molecule clustering reactions are commonly viewed as proceeding via a simple energy transfer mechanism

[11*a*] $C_2H_3^+ + C_2H_2 \rightarrow (C_2H_3^+ \cdot C_2H_2)^*$

[11*b*] $(C_2H_3^+ \cdot C_2H_2)^* + M \rightarrow C_2H_3^+ \cdot C_2H_2 + M$

A strongly negative $T^{(1-s)}$-dependence (where $s$ is the number of internal degrees of freedom involved in "sinking" the excess energy) is observed at low pressures (28), changing to a weak $T^{-1/2}$-(AADO)-dependence at pressure saturation (8). A linear $P$-dependence is observed for the unsaturated process. The saturation pressure is decreased for stronger cluster bonds, for more complex intermediates (larger values of $s$), and for lower temperature. Three "types" of cluster ions may be distinguished on the basis of the strength of the association bond. the weakest type is the simple electrostatic bond, such as that for $O_2^+ \cdot N_2$. These bond dissociation energies are typically $\lesssim 80$ kJ mol$^{-1}$. On the other end of the scale are the strong chemical bonds, such as that observed for $C_2H_3^+ \cdot H_2$ which is indistinguishable from $C_2H_5^+$ derived from the protonation of ethylene (29). Bridging these extremes are the proton-bound intermediates such as $C_2H_3^+ \cdot C_2H_2$ which is a symmetric example.

### 7. *Electron attachment*

Little experimental work has been done on the $T$-dependence of polyatomic electron attachment reactions. The process is generally believed to take place via a modified Bloch–Bradbury mechanism:

[12*a*] $C_nH_x + e^- \rightarrow (C_nH_x^-)^*$

[12*b*] $(C_nH_x^-)^* + M \rightarrow C_nH_x^- + M$

Of the two systems which have been studied in detail, attachment to $O_2$ appears to be well-described by this mechanism, while that to NO is not. This has been explained (30) in terms of the great difference in the lifetimes of the resonant states, $(X^-)^*$; that for $(O_2^-)^*$ is sufficiently long to allow the reaction to be viewed as taking place through two distinct stages, while that for $(NO^-)^*$ is so short that a one-step mechanism must be invoked. However, it may be expected that the energy-transfer (2-step) mechanism is appropriate for the polyatomic $C_nH_x$ hydrocarbons because of the greater number of internal degrees of freedom available to stabilize the intermediate. The kinetics should then be described by the same equations invoked earlier for three-body association reactions. For large molecules having many degrees of freedom, the lifetimes of the intermediates may be long enough to allow the reaction to be characterized as bimolecular (31). Electron affinity (EA) values are known for the $CH_x$ ($x$ = 0–3) species. For higher $C_nH_x$ ($n \geq 2$) species, EA values for the most part are either unknown or uncertain. The stable hydrocarbons have, in general, negative EA's and so electron attachment is an important process only for radical species. It has often been suggested (32) that hydrocarbon anions in flames may result from dissociative attachment reactions. Chief among these is the source proposed for $C_2H^-$

[13] $e^- + C_2H_2 \rightarrow C_2H^- + H$

However, for the thermal electrons of the flames discussed here this reaction is sufficiently endothermic (260 kJ mol$^{-1}$) so as to ensure that its contribution to the observed $C_2H^-$ concentration is minimal. The same conclusion is likely to apply to all stable hydrocarbons. Not enough is known about the energetics of $C_nH_x$ radicals to predict the importance of their dissociative attachment reactions to the negative ionization observed in flames.

### 8. *Associative detachment*

Competing with the thermal detachment of electrons from anions in flames are associative detachment reactions. The relatively large H-atom concentration in hydrocarbon flames facilitates reactions of the type

[14] $C_nH_x^- + H \rightarrow C_nH_{x+1} + e^-$

Most commonly, the product of this reaction is a stable (i.e. non-radical) hydrocarbon molecule. Associative detachment reactions are also expected to be rapid with OH and possibly O. The kinetics may be obtained by applying the principle of detailed balance to dissociative attachment. Since the equilibrium constant may be expected to shift in favor of the reactants ($X^- + H$) as the temperature increases, and the rate constant for dissociative attachment decreases with $T$ (33), the rate constant for associative detachment reactions may be expected to show a slightly negative $T$-dependence. Phelps (33) has argued that for reactions involving a complex which has a short lifetime ($< 10^{-14}$ s) against auto-detaching (such as $O^- + H_2$), the rate constant will be essentially independent of temperature; those having longer auto-detaching lifetimes (such as $O^- + NO$) will demonstrate a weak, approximately $T^{-1/2}$-dependence. Despite the decrease of the rate constant with temperature, the rate of associative detachment reactions in flames may be expected to increase rapidly with temperature in response to the overriding increase in the rate of formation of radicals.

## Discussion

The companion paper I (1) concluded with a summary of the major observations involving positive and negative ion profiles in fuel-rich $CH_4$–$O_2$ flames with, and without, added $C_2H_2$. Much more can be learned about the early chemical stage of soot formation by a detailed consideration of these results in terms of the kinds of ionic reactions given in the previous section which dominate in different regions of these flames: upstream; in the reaction zone proper; and downstream in the burnt gas. This discussion will be presented in accordance with the summary in I; total ionization profiles will be considered first, followed by the behaviour of individual negative ion species, and then positive ion species. Finally, the trends evident in the flame chemistry are discussed as the equivalence ratio $\phi$ is increased at constant temperature towards the sooting point by the addition of acetylene.

### *A. Total ionization profiles*

#### *Positive ions*

The total positive curves in all flames studied show the usual rapid rise through the reaction zone, peaking just downstream, before tailing away through the burnt gas via electron–ion recombination. At constant $\phi$, the peak magnitude shows a positive temperature dependence $T^\beta$ with $\beta \simeq 2.5$ (Fig. 1(*b*) of I). This strong positive $T$-dependence is reasonable for both kinds of source reactions mentioned in the previous section, namely, chemi-ionization and thermal ionization. If the pair of curves with $T_{ad} = 2401$ and 2488 K for $\phi = 2.22 \pm 0.01$ are normalized at the peak, the rising portions through the reaction zone are the same, and there is no shift in peak position. Accordingly, there is no reason to invoke any source reaction other than the usual chemi-ionization process (2, 3)

[1] $CH + O \rightarrow HCO^+ + e^-$

upstream and through the reaction zone. On the other hand, the rate of recombination in the hotter flame is reduced downstream through the burnt gas. Most of the positive charge in this region is present as $H_3O^+$ ions, whose rate of electron–ion recombination

[15] $H_3O^+ + e^- \rightarrow H + H + OH$

has been variously found to have zero $T$-dependence (34) or a $T^{-1.6}$-dependence (35). The downstream behaviour might be accounted for by the negative $T$-dependence. Alternatively, it may possibly indicate the involvement of an additional source term, namely, thermal ionization of carbonaceous radicals of low ionization energy whose presence is expected downstream in these very fuel-rich flames.

#### *Negative ions*

The total negative ion profile in all flames studied is double-peaked. It rises upstream in approximate coincidence with the total positive profile and then breaks away to form a primary maximum midway through the reaction zone. The profile shows a valley near the end of the reaction zone, followed by a secondary maximum just downstream. The magnitude of the upstream peak decreases with increasing $\phi$ (negative $\phi$-dependence) and has little $T$-dependence. This upstream maximum arises because of the relative rates for formation and loss of negative ions, the rates being equal at the peak. The formation process is mainly three-body electron attachment, primarily to $O_2$, while the loss processes include thermal detachment and ion–radical associative detachment reactions, primarily with H atoms in these fuel-rich flames (36). The negative $\phi$-dependence at constant temperature is a consequence of the decrease in the concentration of $O_2$ and increase in H atoms. The apparent lack of $T$-dependence was observed for a pair of flames at constant $\phi$ (Fig. 1(*b*) in I); in the hotter flame, the positive ions increase while the negative ions remain about the same. This relative decrease in negative ion concentration is in keeping with an enhanced rate for both kinds of loss processes; note that the concentration of H increases at higher temperature. However, little of this upstream behaviour provides much insight into the chemical initiation of soot formation.

In contrast, the secondary maximum downstream shows both a strongly positive $\phi$- and $T$-dependence. Also, the negative ion profile in the richer flame tails out considerably further downstream. As discussed below, this behaviour is consistent with an increase in the rate of production of $C_nH_x^-$ ions from hydrocarbon neutrals, for example polyacetylenes or their radicals, whose concentrations increase rapidly with both $\phi$ and $T$. These species must be intimately involved in the initiation of soot.

### *B. Negative ion profiles*

The individual negative ion profile peaks appear in three distinct regions. In the first of these, oxygenated anions are found upstream (e.g. $O^-$, $OH^-$, $O_2^-$, $CH_3O^-$, $O^-{\cdot}H_2O$, $OH^-{\cdot}H_2O$, impurity traces of $^{35}Cl^-$ and $^{37}Cl^-$, $C_2HO^-$, $C_2H_3O^-$, $CHO_2^-$, $O_3^-$, etc., in order of increasing mass, and including $^{13}C$, $^{18}O$, and D isotopically substituted species). These ions are formed by charge transfer from primary $O_2^-$ ions and by proton transfer from parent neutrals by strong bases such as $OH^-$ and $O^-$; every profile peaks close to the $OH^-$, $O^-$, and $O_2^-$ peak positions. In fact, all of the anions with $m/e < 80$ amu can be interpreted as oxygenated species (Fig. 5 of I) with the exception of $C_2H^-$ and possibly a trace of $C_2^-$.

In the second region, a number of moderately unsaturated hydrocarbon anions are observed to peak in the valley region of the total negative ion profile (Figs. 1 and 5 of I). All of these can be interpreted as arising by proton transfer from a stable neutral hydrocarbon, viz. $C_2H^-(C_2H_2)$, $C_3H_3^-(C_3H_4)$, $C_3H_5^-(C_3H_6)$, $C_4H^-(C_4H_2)$, $C_4H_3^-$-$(C_4H_4)$, $C_4H_5^-(C_4H_6)$, and $C_5H_5^-(C_5H_6)$

[16] $OH^- + C_nH_x \rightarrow C_nH_{x-1}^- + H_2O$

In each case, a decreasing concentration of the reagent anion $OH^-$ combined with a rising concentration of the reagent neutral might be expected to yield a maximum product ion concentration in the valley region. It is just possible that the prominent signals at 41, 53, and 65 amu represent a series based on deprotonated ketenes $HC({=}C)_m{=}O^-$ with $m = 1$, 2, and 3, respectively. The important point is that at least some of these peaks in the valley region provide clear evidence for the growth of unsaturated hydrocarbon species as the combustion process proceeds.

In the third region, very highly unsaturated $C_nH_x^-$ ions are observed to peak just beyond the reaction zone, completing a picture of progressive dehydrogenation as the flame chemistry develops. The resultant hydrogen made available appears downstream as $H_2O$ and $H_2$. An important point in the negative ion chemistry is the degree to which it is likely to be free from condensation reactions which complicate the positive ion chemistry. Attention has been drawn to this hypothesis earlier in connection with pure $CH_4$–$O_2$ flames (36). It is important because, if valid, the wide variety of negative ions observed argues in favour of a neutral rather than an ionic mechanism for the buildup of carbonaceous species leading to soot formation.

The whole series of highly unsaturated $C_nH_x^-$ ions in the third region arises near the maximum concentration of free electrons at $z = 0.04 \pm 0.02$ mm. The concentrations of the observed ions alternate with the parity of $n$, the even-$n$ species being larger in agreement with the early observations of Green (37). For $n$ even, the most abundant species are the acetylenic anions $C_2H^-$, $C_4H^-$, $C_6H^-$ ..... with $x = 1$. For $n$ odd, the most abundant ions tend to be those with $x = 0$ and 5 such as $C_3^-$, $C_3H_5^-$, $C_5^-$, and $C_5H_5^-$.

The obvious question concerns the identity of the primary negative ions downstream. The $OH^-$ profile has a secondary maximum at this point in the flame (Fig. 7 of I) which could arise in coincidence with the free electron maximum by dissociative or three-body electron attachment

[17] $e^- + H_2O \rightarrow OH^- + H$

[18] $e^- + OH + M \rightarrow OH^- + M$

The relatively high concentrations of $H_2O$ and OH in this region would favour the rates of reactions [17] and [18]. A strong base such as $OH^-$ would promote chemical ionization of carbonaceous neutrals by proton transfer as in reaction [16]. Secondary ions (e.g. $C_n^-$) can be produced by stripping reactions

[19] $C_nH_x^- + H \rightarrow C_nH_{x-1}^- + H_2$

As an alternative to the proton transfer/stripping mechanism, it is probable that some of the $C_nH_x$ neutrals have positive electron affinities such that three-body and even two-body electron attachment processes may be competitive (31, 36). In general, however, the proton transfer-based mechanism is preferred.

In the $C_4H_x^-$ series, small signals corresponding to $x = 3$, 4, and 5 were also observed (Fig. 2(*b*) of I) which could arise by proton abstraction from dimethylacetylene followed by H atom stripping. This mechanism is thought to be more likely than hydrogenation of the highly unsaturated species, for example, by the reverse of reaction [19], although the thermochemistry is not known.

Methylpolyacetylenes $C_nH_4$ or the isomeric polyallenes can lead to ionic species with $n$ odd, but impose a limit on $x \leq 4$. In the lower series with $n = 3$ and 5, the ionic concentrations increase with decreasing $x$, and the ions with $x = 4$ are not observed. Presumably the same combination of proton transfer followed by H atom stripping reactions is involved as with $n$ even. However, these parent molecules do not explain the origin of the relatively large signals observed for $n$ odd with $x = 5$. The $C_nH_5^-$ ions are thought to arise by proton abstraction from $C_nH_6$ species derived, for example, by $H_2$ elimination reactions of polyacetylenes with propylene, or methylpolyacetylenes with ethylene.

Note that these schemes provide a probable explanation for the observed intensity alternation with the parity of $n$ (Fig. 2(*a*) in I). Both the $C_nH_4$ and $C_nH_6$ parent neutrals invoked for the ions with $n$ odd are secondary reaction products of the basic polyacetylenes responsible for the larger ion signals observed with $n$ even. For a given $n$, the concentrations of the secondary derivatives would be expected to be less than the concentration of the corresponding primary reagent. The main reason for exploring this negative ion chemistry in some depth is to show that all of it can be based on acetylene. The early chemical stage leading to soot formation appears overwhelmingly to involve neutral condensation (polymerization) reactions of acetylene, the negative ions serving as a probe. Implicit in this discussion has been the notion that a negative chemical ionization process applied to a neutral flame intermediate preserves the identity of that neutral by producing an ion of the same, or nearly the same, mass.

### *C. Positive ion profiles*

The positive hydrocarbon ions $C_nH_x^+$ form a number of series through the flame reaction zone defined by the value of $n$ with $0 \leq x \leq 10$ (Fig. 2(*c*) of I). In each series, the profile peak positions evolve downstream with decreasing values of $x$ amounting to progressive dehydrogenation (Figs. 3 and 4 of I). Also within each series, the peak magnitudes (*a*) tend to be larger for small values of $x$, (*b*) maximize for $x = 3$, and (*c*) show a measure of alternation with the parity of $x$, odd $x$ being larger. Overall, the series are remarkably similar such that the positive ion chemistry appears to be essentially independent of $n$.

To what degree are these positive ions formed by simple CI processes (e.g. proton transfer, charge transfer, etc.) involving large hydrocarbon neutrals? Or, do they merely result from fast, ion–molecule condensation reactions which reveal little about the buildup of carbonaceous precursors to soot formation? Or possibly the ion–molecule condensation reactions are themselves competitive, with implications for an ionic mechanism of soot formation? These are the questions this discussion attempts to answer by considering the kinds of positive ion–molecule reactions likely to be involved, by making use of published data available for individual ion–molecule reactions given in Tables 2–4, and by seeking a correlation with the negative ion data.

#### *Thermal ionization*

This process can be discounted as a significant ion source in ordinary hydrocarbon flames (38). There is no known constituent of sufficient concentration and low enough ionization energy (IE) to yield a reasonable ion density even at equilibrium, and the kinetics are too slow for equilibrium to be approached in the flame reaction zone. Nevertheless, it is worth noting for aliphatic $C_nH_x$ radicals and molecules the trends in IE with $n$ and $x$ given in Fig. 1. The obvious feature is the alternation of IE with $x$; IE's of odd-$x$ species are roughly 1.5 eV lower than those of similar species with even-$x$. This, of course, describes quite well the alternation observed in the positive ion mass spectrum. Also, the IE tends to decrease with increasing $n$ (except for $x = 0$). We have estimated the concentration of $C_4H_5^+$ from thermal ionization of $C_4H_5$ radicals present with a mole fraction of $10^{-5}$ at the adiabatic flame temperature $T_{ad} = 2455$ K for a flame with $\phi = 2.15$. The calculated density of $1 \times 10^8$ ions cm$^{-3}$ agrees very well with the maximum concentration measured for $C_4H_5^+$, based on an estimate of $4 \times 10^{10}$ ions cm$^{-3}$ for the peak of the total positive ionization curve (39). This model can be discounted upstream in the reaction zone where the temperature $< T_{ad}$ because of the strong positive $T$-dependence for thermal ionization. Nevertheless, it may possibly represent a competitive process for hydrocarbonaceous ion formation downstream in the burnt gas. This is the source process mentioned in Section A on total ionization profiles to explain the apparent decrease in the rate of electron–ion recombination observed with increasing $\phi$ and $T$.

#### *Three-body association*

The bond-dissociation energies of electrostatically-bound ion–molecule clusters are expected to increase with increasing dipole moment of the neutral. The relatively low dipole moments of the hydrocarbon intermediates, the difficulty in explaining the observed intensity alternation with $x$, and the failure to account for the dehydrogenation series for a given $n$ all argue against any major contribution from three-body association. Certainly in the hot part of the flame, the strong negative $T$-dependence of these reactions renders them unlikely. A somewhat greater contribution might be expected in the cooler domain far upstream except that oxygenated hydrocarbons would be preferred as clustering agents in this region for reasons of higher dipole moment and concentration. Similar considerations apply to three-body association reactions leading to the formation of hydrogen-bonded or chemically-bonded adducts even though their rates may be higher.

*Condensation*

Many of the smaller hydrocarbon ions have been observed to undergo condensation reactions having high rate constants at room temperature with both elements of the fuel, $CH_4$ and $C_2H_2$, as is evident from Tables 2 and 3. A condensation-dominated ion chemistry might explain the positive ion $n$-series to some extent. Complications arise because a number of the hydrocarbon ions can participate in rapid, exothermic, *hydrogenation* reactions even at room temperature as given in Table 4. Molecular hydrogen is available as a reagent since it becomes a major combustion product downstream in these fuel-rich flames. Ion–molecule condensation reactions will be occurring throughout the flame with simultaneous dehydrogenation, e.g. reaction types ($a$), ($b$), ($c$), ($g$), ($h$), and ($j$) given in Tables 2 and 3, although the extrapolation of this data base to flame temperatures and higher-$n$ ions is uncertain. However, the limited room temperature data are of little help in explaining the intensity alternation with $x$. On the other hand, the similarity of the various $n$-series is consistent with ubiquitous condensation reactions involving the same neutral reagents, namely, $CH_4$ and $C_2H_2$.

*Charge transfer*

Charge transfer reactions cannot explain the rapid buildup of hydrocarbon ions of high molecular weight. If charge transfer plays a major role, it presupposes the neutral polymerization of the fuel early in the flame. From Fig. 1, the lower IE's of the $C_nH_x$ neutrals having odd $x$ mean that charge transfer is the best mechanism available to account for the measure of intensity alternation (Fig. 2($c$) of I) observed within each $n$-series. It is significant that, typically, $\mathrm{IE}(C_nH_x, x \text{ odd}) < \mathrm{IE}(HCO) \simeq 8.7$ eV $< \mathrm{IE}(C_nH_x, x \text{ even})$, such that charge transfer reactions of primary $HCO^+$ ions are exothermic with many odd-$x$ species formed by fuel pyrolysis. These reactions may be fast enough to deplete the $HCO^+$ as rapidly as it is formed, in keeping with the failure to observe significant amounts of $HCO^+$ far upstream where $C_nH_x^+$ ions are prominent. If a charge transfer mechanism is truly dominant, the initial neutral pyrolysis products must undergo sequential dehydrogenation via the *neutral* flame chemistry; the $C_nH_x^+$ series would then evolve by progressive charge transfer to the dehydrogenation intermediates.

*Proton transfer*

The data base of known PA's for $C_nH_x$ species given in Table 1 is insufficient to identify any clear-cut trends with $n$ and $x$, although the PA appears to increase with the degree of unsaturation (increasing C/H ratio). However, a proton transfer mechanism is consistent with the observed intensity alternation with $x$ within each $n$-series. Even-$x$ hydrocarbon neutrals (except for $x = 0$) almost always correspond to stable molecules which will tend to be present in higher steady-state concentrations in the flame, unlike odd-$x$ species which are always free radicals. Obviously, even-$x$ neutrals protonate to form odd-$x$ ions.

If the positive ion chemistry is dominated by proton transfer, it presupposes that the neutral chemistry involves an initial pyrolysis stage with condensation followed by progressive dehydrogenation. The latter is expected to proceed mainly via H atom abstraction in such a fuel-rich flame. The terminal stable member of each $n$-series of neutrals from a point of view of dehydrogenation is a polyacetylene which must await oxidative cleavage or neutral condensation. This may explain the maximum for $x = 3$ obtained in each $n$-series of ions. Also, this chemical scheme (neutral pyrolysis with condensation, ionic proton transfer) provides a consistent basis for the observed similarity of the various $n$-series of ions.

### *D. The influence of $C_2H_2$ added to the $CH_4$ fuel*

The results discussed in Sections B and C pertain to a $CH_4$–$C_2H_2$–$O_2$ flame (17.7% $C_2H_2$) with $\phi = 2.47$ in which traces of yellow soot luminescence could be seen around the cooler perimeter. However, similar profile data were also measured for a leaner $CH_4$–$O_2$ flame without added $C_2H_2$ having $\phi = 2.15$ burning at the *same temperature*. When the data from the richer flame are compared with those from the leaner, most of the differences are entirely consistent with decreased C/O and increased C/H ratios (point 6 in the summary of I): unsaturated $C_nH_x^{\pm}$ ion signals increase at the expense of oxygenated ions upstream; the ion profile peaks become broader (it was suspected that the reaction zone thickness had increased) and more skewed in the downstream directions (e.g., $C_3H_3^+$ in Fig. 8 of I); positive ions having high $n$ and low $x$ values are enhanced.

In a relatively few isolated cases, profile peak magnitudes in the reaction zone showed a considerable decrease with added $C_2H_2$ (at +15, +49, +61, −17, and −60 amu from Figs. 6 and 7 of I). Some of these are readily understandable in terms of known fast reactions with $C_2H_2$ which have been measured at room temperature; for example

[20] $CH_3^+ + C_2H_2 \rightarrow C_3H_3^+ + H_2$ (23)

[21] $OH^- + C_2H_2 \rightarrow C_2H^- + H_2O$ (6)

Somewhat surprisingly, however, the two sets of profiles obtained for the two flames were remarkably similar as to relative peak heights, positions, and shapes. Evidently the identities of the fuel molecules are essentially lost early in the reaction zone through pyrolysis and decomposition processes. Even the upstream peaks of the $C_2H^-$ and $C_2H_3^+$ profiles (Figs. 7 and 8 of I) which are closely related to acetylene did not respond greatly to the addition of 17.7% of $C_2H_2$. In fact, the significant change at −25 amu was the appearance of an additional shoulder in a position *intermediate* between the upstream and downstream peaks. This shoulder is indicative of $C_2H_2$ synthesis in the reaction zone subsequent to the disappearance of the original $C_2H_2$ fuel. Thus, these results with varying $\phi$ at constant temperature provide additional evidence that the fuel undergoes pyrolysis very early in the flame.

## Conclusions

The total ionization profiles, both positive and negative, in these fuel-rich flames were examined with regard to their $T$-dependence, $\phi$-dependence, profile shape, peak position, and possible source and sink reactions. The positive profiles are consistent with a major chemi-ionization source reaction upstream persisting through the reaction zone, and possibly a minor source term downstream arising from thermal ionization of hydrocarbon radicals of low ionization energy. This latter source term may well become dominant as the flame is made increasingly fuel-rich (40). The behaviour of the negative profiles is consistent with electron attachment to oxygen upstream, and hydrocarbon ion production downstream in the burnt gas based on the presence of carbonaceous neutral species.

Individual negative ion profiles correspond to oxygenated anions upstream. Further downstream in the reaction zone, in a region corresponding to a valley in the total negative ion profile, several profiles show peaks representative of moderately unsaturated hydrocarbon anions. They appear to be formed by proton transfer from stable hydrocarbon neutrals, and are resistant to destruction by associative detachment with H atoms. They are important because they illustrate the growth of unsaturated hydrocarbon species originating in the reaction zone. The progressive dehydrogenation continues downstream in the burnt gas giving rise to highly unsaturated carbonaceous anions which appear to be formed by proton abstraction from corresponding neutrals by $OH^-$ and H atom stripping. An important point is the degree to which negative ions participate in ion–molecule condensation reactions; if minimal, the observations argue for neutral condensation as the mechanism responsible for the buildup of large carbonaceous species leading to soot formation. Note that all of the negative hydrocarbon ions can be explained in terms of polyacetylene derivatives; we favour the idea that methylpolyacetylenes and not allenic derivatives are responsible for the intensity alternation observed for $C_nH_x^-$ ions (lower for $n$ odd).

Individual positive profiles for $C_nH_x^+$ ions have been considered in the light of several kinds of ion–molecule reactions. The relative contributions of the different kinds can be judged to some extent from observations on progressive dehydrogenation downstream, intensity maxima for $x = 3$, $x$ intensity alternation, the great similarity of different $n$ series, and considerations involving magnitudes of measured rate constants, $T$-, $\phi$-, and $P$-dependence, and the dependence of IE on $n$ and $x$ (see Fig. 1). On these bases, we conclude that proton transfer reactions play a major role throughout the flame in the chemical ionization of neutral species and, to a lesser extent, charge transfer. These mechanisms presuppose extensive fuel pyrolysis early in the reaction zone, and a backbone of neutral polymerization chemistry resulting in the formation of large carbonaceous species, the precursors of soot. Ion–molecule condensation reactions must also be occurring but appear to be of lesser importance; perhaps such reactions involving methane are responsible for masking the intensity alternation with $n$ which is a major feature of the negative ion spectrum (see Fig. 2 of I). Thermal ionization will not be competitive in these flames except perhaps for a minor contribution downstream in the burnt gas. Finally, the role of three-body association reactions is probably insignificant in view of the observations and considerations outlined above.

Many of these notions are reinforced by the experiments in which acetylene was added to the methane fuel. In general, the fact that nearly all of the ion profiles, both positive and negative, are remarkably unaffected by acetylene provides additional evidence for early fuel pyrolysis. As a general conclusion based on these studies of the early chemical stages leading to soot formation, the ion–molecule chemistry might conceivably make some contribution but is not thought to be dominant compared with neutral mechanisms involving polymerization of the fuel. Because of complexities associated with the positive ion chemistry, we believe that the negative ion profiles give the better picture of the chemical growth towards soot formation, the negative ions merely serving as a probe of the underlying neutral chemistry.

1. S. D. TANNER, J. M. GOODINGS, and D. K. BOHME. Can. J. Chem. **59**, 1760 (1981).
2. H. F. CALCOTE. Eighth Symposium (International) on Combustion, Williams and Wilkins, Baltimore, MD. 1962. p. 184.
3. K. N. BASCOMBE, J. A. GREEN, and T. M. SUGDEN. Adv. Mass Spectrom. **2**, 66 (1962).
4. A. FONTIJN. Prog. Reaction Kinet. **6**, 75 (1971).
5. R. E. WESTON and H. A. SCHWARA. Chemical kinetics. Prentice-Hall, Englewood Cliffs, NJ. 1972. p. 130.
6. G. I. MACKAY, K. TANAKA, and D. K. BOHME. Int. J. Mass Spectrom. Ion Phys. **24**, 125 (1977).
7. S. D. TANNER, G. I. MACKAY, and D. K. BOHME. Can. J. Chem. **59**, 1615 (1981).
8. T. SU, E. C. F. SU, and M. T. BOWERS. J. Chem. Phys. **69**, 2243 (1978).
9. R. WALDER and J. L. FRANKLIN. Int. J. Mass Spectrom. Ion Phys. **36**, 85 (1980).
10. H. M. ROSENSTOCK, K. DRAXL, B. W. STEINER, and J. T. HERRON. J. Phys. Chem. Ref. Data, **6**, (1977), Supplement 1.
11. G. B. DEBROU, J. E. FULFORD, E. G. LEWARS, and R. E. MARCH. Int. J. Mass Spectrom. Ion Phys. **26**, 345 (1978).
12. G. I. MACKAY and D. K. BOHME. Int. J. Mass Spectrom. Ion Phys. **26**, 327 (1978).
13. J. B. HOPKINS, D. E. POWERS, and R. E. SMALLEY. J. Chem. Phys. **74**, 6985 (1981).
14. K. TANAKA, G. I. MACKAY, and D. K. BOHME. Can. J. Chem. **56**, 193 (1978).
15. D. K. BOHME and G. I. MACKAY. J. Am. Chem. Soc. **103**, 2173 (1981).
16. D. K. BOHME, G. I. MACKAY, and H. I. SCHIFF. J. Chem. Phys. **73**, 4976 (1980).
17. D. K. BOHME, G. I. MACKAY, H. I. SCHIFF, and R. S. HEMSWORTH. J. Chem. Phys. **61**, 2175 (1974).
18. G. I. MACKAY, H. I. SCHIFF, and D. K. BOHME. Can. J. Chem. **59**, 1771 (1981).
19. N. G. ADAMS and D. SMITH. Chem. Phys. Lett. **47**, 383 (1977).
20. R. S. HEMSWORTH, R. C. BOLDEN, M. J. SHAW, and N. D. TWIDDY. Chem. Phys. Lett. **5**, 237 (1970).
21. L. W. SIECK and S. G. LIAS. J. Phys. Chem. Ref. Data, **5**, 1123 (1976).
22. D. SMITH and N. G. ADAMS. Int. J. Mass Spectrom. Ion Phys. **23**, 123 (1977).
23. D. SMITH and N. G. ADAMS. Chem. Phys. Lett. **54**, 535 (1978).
24. J. A. BURT, J. L. DUNN, M. J. MCEWAN, M. M. SUTTON, A. E. ROCHE, and H. I. SCHIFF. J. Chem. Phys. **52**, 6062 (1970).
25. D. SMITH and N. G. ADAMS. Astrophys. J. **217**, 741 (1977).
26. F. C. FEHSENFELD, D. B. DUNKIN, and E. E. FERGUSON. Astrophys. J. **188**, 43 (1974).
27. H. I. SCHIFF and D. K. BOHME. Int. J. Mass Spectrom. Ion Phys. **16**, 167 (1975).
28. D. SMITH and N. G. ADAMS. Astrophys. J. (Lett.), **220**, L87 (1978).
29. S. D. TANNER, G. I. MACKAY, and D. K. BOHME. Can. J. Chem. **57**, 2350 (1979).
30. G. E. CALEDONIA. Chem. Rev. **75**, 333 (1975).
31. L. G. CHRISTOPHOROU. Atomic and molecular radiation physics. Wiley-Interscience, London. 1971. p. 500.
32. A. N. HAYHURST and D. B. KITTELSON. Combust. Flame, **31**, 37 (1978).
33. A. V. PHELPS. Can. J. Chem. **47**, 1783 (1969).
34. A. N. HAYHURST and N. R. TELFORD. J. Chem. Soc. Faraday Trans. I, **70**, 1999 (1974).
35. R. KELLY and P. J. PADLEY. Trans. Faraday Soc. **66**, 1127 (1970).
36. J. M. GOODINGS, D. K. BOHME, and C.-W. NG. Combust. Flame, **36**, 45 (1979).
37. J. A. GREEN. 26th AGARD Propulsion and Energetics Panel, Pisa, Italy, AGARD Conference Proceedings No. 8. Vol. I. Edited by H. D. Wilsted. 1965. p. 191.
38. H. F. CALCOTE. Combust. Flame, **1**, 385 (1957).
39. J. M. GOODINGS, D. K. BOHME, and C.-W. NG. Combust. Flame, **36**, 27 (1979).
40. J. L. DELFAU, P. MICHAUD, and A. BARASSIN. Combust. Sci. Technol. **20**, 165 (1979).